10042 Vol. 60, No. 32 / 10 November 2021 / *Applied Optics* **Research Article**

applied optics

Second-harmonic and sum-frequency generation based on birefringence phase matching of $BaMgF_4$ crystal

SHUO YAN,[1,†] ZHANWEI LIU,[1,†] HAIGANG LIU,[1] YIWEI SUN,[1] YUANLIN ZHENG,[1,2,5] AND XIANFENG CHEN[1,2,3,4,*]

[1] *State Key Laboratory of Advanced Optical Communication Systems and Networks, School of Physics and Astronomy, Shanghai Jiao Tong University, Shanghai 200240, China*
[2] *Shanghai Research Center for Quantum Sciences, Shanghai 201315, China*
[3] *Jinan Institute of Quantum Technology, Jinan 250101, China*
[4] *Collaborative Innovation Center of Light Manipulation and Applications, Shandong Normal University, Jinan 250358, China*
[5] *e-mail: ylzheng@sjtu.edu.cn*
**Corresponding author: xfchen@sjtu.edu.cn*

Received 20 August 2021; revised 16 October 2021; accepted 17 October 2021; posted 18 October 2021 (Doc. ID 438688); published 2 November 2021

$BaMgF_4$ is a ferroelectric nonlinear crystal with a very wide transparency window ranging from 125 nm to 13 μm of the wavelength. Therefore, it is a candidate material to generate ultraviolet or deep ultraviolet laser, which is very important in lithography, semiconductor manufacturing, and advanced instrument development. Here, the second-order birefringence phase-matching processes of the $BaMgF_4$ crystal were studied, including second-harmonic generation (SHG) and sum-frequency generation (SFG). In the experiments, we measured the phase-matching angle, nonlinear frequency conversion efficiency, and angle bandwidth of SHG and SFG processes of $BaMgF_4$ crystal, which are in well agreement with the theoretical calculations. This study may promote the research of nonlinear optical process of $BaMgF_4$ crystal and also the further development of all-solid-state vacuum ultraviolet lasers.

https://doi.org/10.1364/AO.438688

1. INTRODUCTION

Coherent vacuum ultraviolet (VUV, wavelength $\lambda < 200$ nm) light sources are of great interest in modern laser science and technology, such as imaging, spectroscopy, and optical communications [1–8]. Presently, excimer lasers such as ArF (193 nm) and KrF (248 nm) are mainly used in the UV wavelength region [9,10]. However, these excimer lasers have several disadvantages such as fast degradation, toxicity, and low beam quality [11]. Therefore, researchers have proposed to produce VUV light sources assisted by the frequency conversion of nonlinear optical (NLO) materials [12–14], which is a method to circumvent the abovementioned problems of excimer lasers. The VUV NLO material should have a bandgap larger than 6.2 eV, large SHG coefficient, and sufficient birefringence to ensure phase matching in the VUV wavelength range [15–18]. The widely used NLO borate crystals LiB_3O_5 [19], $\beta - BaB_2O_4$ [18,20], and $KBe_2BO_3F_2$ (KBBF) [21] are featured by relatively strong SHG coefficient with moderate birefringence. The KBBF has a VUV cutoff wavelength of 150 nm with a rather moderate birefringence value of 0.077 [5]. It is a popular NLO material to generate laser with VUV wavelengths [22]. However, KBBF crystals have a strong layered structure, and it is very easy to crack along the *c* axis during the growth process. The crystal is too thin to be cut along the phase-matching direction for producing deep UV harmonic generations beyond 200 nm [23]. Since the 1990s, with the emergence and development of polarization technology at room temperature, a series of ferroelectric fluoride crystals with short UV absorption edges discovered in the middle of the last century have received attention, among which the most representative is the crystal of barium magnesium fluoride ($BaMgF_4$) [24]. The transmission range of $BaMgF_4$ crystal is from 125 nm to 13 μm, which is a VUV ultratransparent crystal. It is one of the strong candidates for generating VUV all-solid-state lasers [25]. In addition, the $BaMgF_4$ crystal is a ferroelectric crystal. The quasi-phase-matching (QPM) method can take full advantage of the wide transparency of $BaMgF_4$ in the UV wavelength region [21]. The two-dimensional nonlinear photonic structure of $BaMgF_4$ is also possible to generate nonlinear harmonic waves in multiple wavelengths and directions [26]. However, experiment on the second-order birefringence phase-matching process of $BaMgF_4$ have still been not studied.

In this paper, we theoretically and experimentally studied the second-order birefringent phase-matching process (SHG and SFG) of the $BaMgF_4$ crystal. We observed SHG with the wavelength of 375–550 nm and measured the SH intensity, nonlinear frequency conversion efficiency, and the angular bandwidth with the increase of the fundamental frequency (FF) light, which are in good agreements with the theoretical prediction. The shortwave limit of the birefringent phase matching should be 573 nm of the FF wavelength through the phase-matching theory. However, since the effective nonlinear coefficient at FF wavelength 573 nm is 0, the SHG process did not appear. Besides, we did not effectively detect the SHG when the wavelength was less than 375 nm because of the relative smaller effective nonlinear coefficient. We also measured the SF intensity and the angle bandwidth of the SFG process by using 1152 and 576 nm laser in the $BaMgF_4$ crystal, which are well in agreement with the theoretical calculations.

2. RESULTS AND DISCUSSION

In our experiment, the $BaMgF_4$ bulk crystal is grown by the Bridgman–Stockbarger method [27], which cut along the optical main axis direction with the size of 0.7 cm × 1 cm × 1.3 cm as shown in Fig. 1(a). The schematic of the SHG process experimental setup is shown in Fig. 1(b). In the experiment, a nanosecond laser with wavelength tunable from 400 to 2000 nm is used. The light emitted from the laser is focused on the $BaMgF_4$ crystal after adjusting the intensity and polarization by using a half-wave plate (HWP) and Glan–Taylor prism (GTP), which is not shown in Fig. 1(b). A precision rotating table is used to rotate the angle of the $BaMgF_4$ crystal. After the $BaMgF_4$ crystal, a prism is used to separate the light with different wavelengths. The SHs with the wavelengths of 375–550 nm are detected on the screen. Part of the experimental results are shown in Fig. 1(c), which are, respectively, corresponding to 550, 525, 500, 475, 425, and 375 nm for the SH.

We further measured the change of the SH intensity with the variation of FF light intensity. The SH intensity can be expressed as

$$I_{SH} \propto |I_0|^2 (d_{\text{eff}} L/(2\pi\lambda))^2 \sin c^2 (\Delta k L/2), \qquad \textbf{(1)}$$

where I_0 is the FF light intensity, L is the crystal length, λ is the wavelength of the FF light, d_{eff} is the effective nonlinear coefficient of $BaMgF_4$ crystal, and $\Delta k = 2k_1 - k_2$ is the phase mismatching between the wavevector of FF (k_1) and SH waves (k_2). In case of the birefringence phase-matching process, there is a squared relationship between the SH wave intensity and the FF light intensity. Without loss of generality, we measured the power changing of the SHG with the increase of FF power at the wavelengths of 750, 850, 950, and 1050 nm, which is shown in Fig. 2(a). The experimental results are in good agreement with the theoretical predictions corresponding to Eq. (1). Besides, we rotated angle of $BaMgF_4$ crystal around the phase-matching angle to detect its angle bandwidth with the FF wavelength of 750 nm. The relationship between the SH intensity and the incident angle of the FF light α is shown in Fig. 2(b), which is in good agreement with the theoretical prediction according to Eq. (1). Besides, the SHG efficiency at the phase-matching condition is shown as

$$\eta_{SH} = |I_{SH}|/|I_0| = |I_0| (d_{\text{eff}} L/(2\pi\lambda))^2. \qquad \textbf{(2)}$$

We measured the nonlinear frequency conversion efficiency of the SHG processes with FF wavelength of 750, 850, 950, and 1050 nm, which is shown in Fig. 2(c). We can see that the nonlinear conversion efficiency has a linear correlation with the FF power, which is in good agreement with the theory.

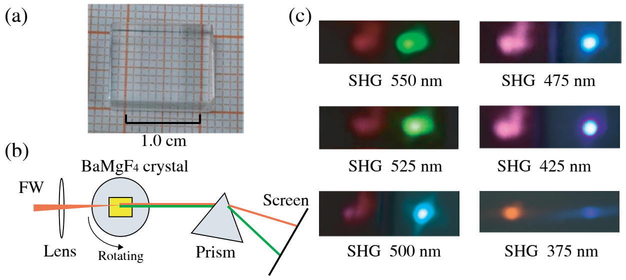

Fig. 1. (a) $BaMgF_4$ crystal grown by the Bridgman–Stockbarger method. (b) Schematic of the experimental setup for SHG. (c) Experimental results of the SHG with the wavelengths of 550, 525, 500, 475, 425, and 375 nm.

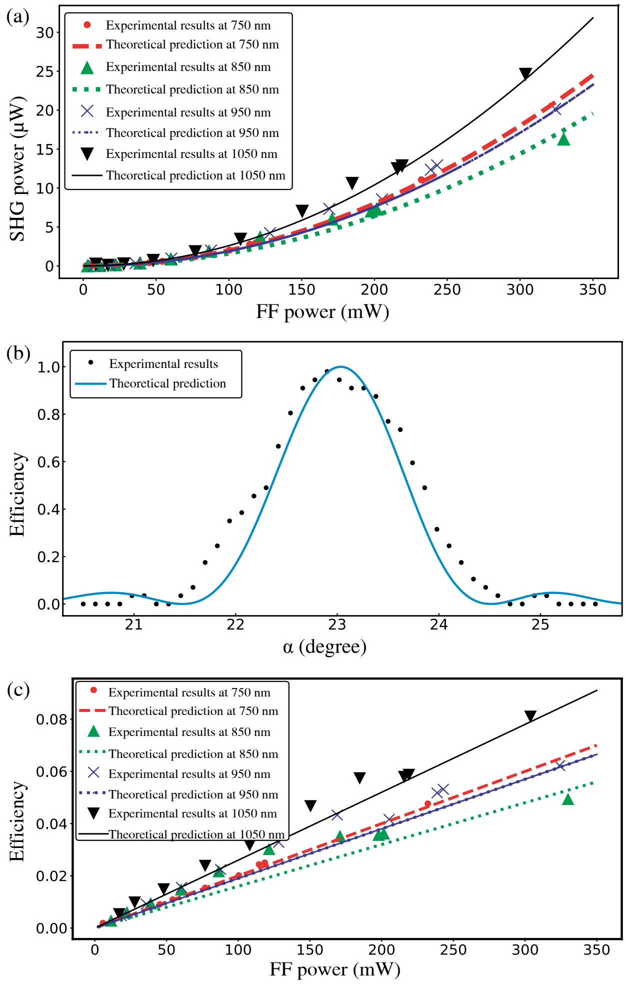

Fig. 2. (a) Relationship between SH power and input FF light power. (b) Angle bandwidth of the SHG process. (c) SH efficiency in our experiment with FF wavelengths of 750, 850, 950, and 1050 nm.

BaMgF$_4$ is a biaxial crystal [28], and the refractive index n_i along the wave vector direction can be calculated by

$$\frac{k_x^2}{(n_i^{-2}-n_{ix}^{-2})}+\frac{k_y^2}{(n_i^{-2}-n_{iy}^{-2})}+\frac{k_z^2}{(n_i^{-2}-n_{iz}^{-2})}=0, \qquad (3)$$

where k_x, k_y, and k_z represent the projection of the wave vector of light on the main axis. n_{ix}, n_{iy}, and n_{iz} represent the refractive index on the main axis. In the spherical coordinate system, the component of the incident light wave vector k along the three main axis directions can be written as $k_x = \sin(\theta)\cos(\phi)k$, $k_y = \sin(\theta)\sin(\phi)k$, and $k_z = \cos(\theta)k$, where θ is the angle between the k and z axes, and ϕ is the angle between the k projection in the $x-o-y$ plane and the x axis. By solving Eq. (3), two solutions n_f and n_s can be obtained, which represent the large and small refractive index, respectively.

In BaMgF$_4$ crystals, the phase-matching method can be specifically divided into type I (ss-f) and type II (sf-f), which correspond to $n_1^s\omega_1 + n_2^s\omega_2 = n_3^f\omega_3$ (type I) and $n_1^s\omega_1 + n_2^f\omega_2 = n_3^f\omega_3$ (type II). The relationship between θ and ϕ under the condition of birefringence phase matching can be numerically solved as shown in Fig. 3. The theoretical shortwave limit is 573 nm of the FF light wavelength as shown by point A in Fig. 3. However, we only detected the SHG within the FF light wavelength range of 750–1200 nm in our experiment. That is because the effective nonlinear coefficient of the BaMgF$_4$ crystal is 0 near point A in Fig. 3. In the $y-z$ plane ($\theta = \pi/2$), the effective nonlinear coefficient of the phase-matching type I (zz-e) can be written as $d_{\text{eff}} = d_{23}\cos(\phi)$ [29]. Therefore, we did not effectively detect the SHG when the wavelength is less than 375 nm because of the relatively smaller effective nonlinear coefficient aroused by the smaller ϕ. In addition, the type I (ee-x) does not exist because the effective nonlinear coefficient is 0 in the $x-z$ plane ($\phi = \pi/2$). In our experiments, the phase-matching angles of the SHG are coincident with the theoretical prediction.

In order to further shorten the emitted wavelength of BaMgF$_4$ crystals, SFG experiments are conducted. The schematic of our experimental setup for SFG in BaMgF$_4$ crystal is shown in Fig. 4(a). We use the nanosecond laser with the wavelength of 1152 nm as the incident light. The FF light is focused on the LiNbO$_3$ (LN) crystal to generate the laser with wavelength of 576 nm. The FF light and SHG with wavelength of 1152 and 576 nm are focused on the BaMgF$_4$ crystal at the same time to produce the SFG. According to the calculation, the phase-matching angle is almost near the main axis of BaMgF$_4$ crystal in this case. The BaMgF$_4$ crystal is cut along the main axis direction in the SFG process. Therefore, these two light beams can increase the overlap during propagation inside the BaMgF$_4$ crystal to produce high-efficiency SFG. Finally, the light beam is split by the prism and is analyzed by the light screen and a spectrometer. The wavelengths of FF, SHG, and SFG are 1152, 576, and 384 nm, respectively. The SFG experiment results of the SHG and SFG light with wavelength 576 nm and 384 nm are shown in Fig. 4(b). The spectrum of light is shown in Fig. 4(c).

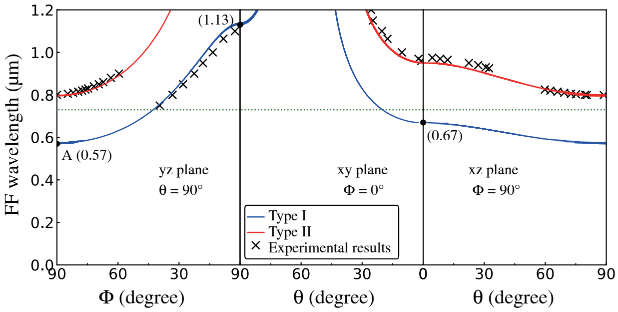

Fig. 3. Theoretical and experimental comparison of SHG phase-matching angle in BaMgF$_4$ crystal.

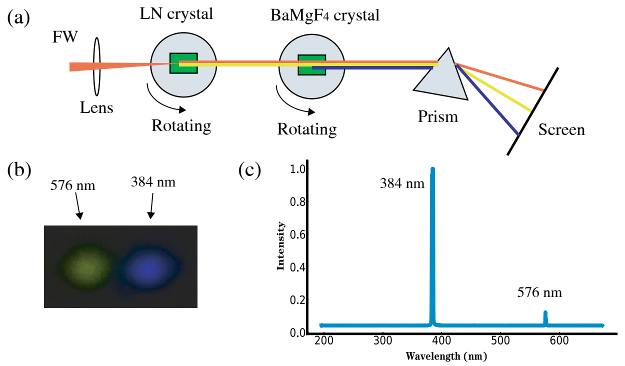

Fig. 4. (a) Schematic of the experimental setup for SFG. (b) SFG experiment results of the SHG and SFG light with wavelength 576 and 384 nm. (c) Spectrum of light with wavelength of 576 and 384 nm.

The intensity of SFG light can be expressed as

$$I_{\text{SF}} = \frac{(8\omega_3^2 d_{\text{eff}}^2 I_1 I_2 L^2)}{n_1 n_2 n_3 c^3 \epsilon_0} \sin c^2(\Delta kL/2) \propto |I_1|^3, \qquad (4)$$

where I_1 is the input light intensity of 1152 nm. ω_3 is the frequency of SFG. I_2 is the light intensity of 576 nm, which is the SHG output generated after LiNbO$_3$ crystal. n_1, n_2, n_3 are the refractive indexes corresponding to the three lights. c is the speed of light in a vacuum. is the vacuum dielectric constant. We also calculated and experimentally obtained the angle bandwidth in the SFG experiment and plotted the relationship between the intensity of SFG light with the angle of the crystal as shown in Fig. 5(a). The relationship between the normalized SFG intensity and the phase mismatch angle β is the square of the sinc function. In addition, we also measure the change of the normalized SFG intensity with the input power of FF light, which is shown in Fig. 5(b). The relationship between the SFG signal and the FF light also presents a cubic relationship, which is in good agreement with the experiment.

We have carried out a detailed study on the SHG and SFG of the vacuum ultraviolet ultratransparent crystal BaMgF$_4$ experimentally for the first time as far as we know. This study further

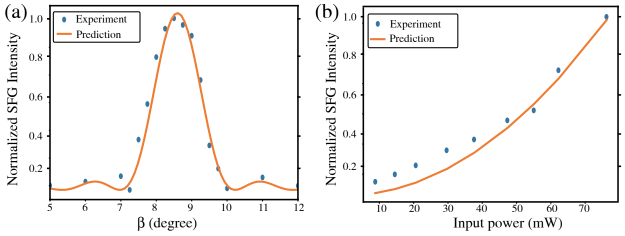

Fig. 5. (a) Angle bandwidth of the SFG process. (b) Relationship between normalized SFG intensity with increase of the FF power.

confirmed the correctness of the SHG phase-matching theory. The SHG intensity, angle bandwidth, and conversion efficiency are in good agreement with the theoretical predictions. The realization of the sum-frequency process also makes it feasible to use $BaMgF_4$ crystalsto generate lasers closer to VUV.

The second-order birefringence phase matching of the $BaMgF_4$ crystal studied in this paper can fully confirm its nonlinear optical properties, which promote the research of nonlinear optical process of $BaMgF_4$ crystal and lay the foundation of UV lasers. In the future, the $BaMgF_4$ crystal is expected to realize VUV waveband harmonic generation by using its ferroelectric property to achieve quasi phase matching (QPM) in periodically polarized crystal. Therefore, the highly compact VUV laser based on $BaMgF_4$ crystal can bring significant applications in imaging, spectroscopy, and optical microfabrication in the future.

3. CONCLUSION

We experimentally studied the second-order birefringence phase-matching processes of the vacuum ultraviolet ultratransparent crystal $BaMgF_4$, including SHG and SFG. The SH with the wavelength of 375–550 nm are observed. Without the loss generality, we measured the SH intensity, nonlinear frequency conversion efficiency, as well as the angular bandwidth with the intensity increasing of the FF light at some fixed wavelength, which are in good agreement with the theoretical prediction. According to the theoretical prediction, the shortwave limit of the birefringence phase matching should be 573 nm of the FF wavelength. However, we did not observe the SH radiation because the effective nonlinear coefficient is 0 at 573 nm of the FF wavelength. Besides, we did not effectively detect the SHG when the wavelength is less than 375 nm because of the relatively smaller effective nonlinear coefficient. In addition, we measured the SFG process of the $BaMgF_4$ crystal by using 1152 and 576 nm lasers. The normalized SF intensity and the angle bandwidth are measured with the changing of the incident light power, which are also in good agreement with the theoretical prediction. This study may promote the research of nonlinear optical processes of $BaMgF_4$ crystal and also the further development of all-solid-state vacuum ultraviolet lasers.

Funding. National Key Research and Development Program of China (2017YFA0303701, 2018YFA0306301); National Natural Science Foundation of China (11734011, 12004245, 12074252, 62022058); Shanghai Municipal Science and Technology Major Project (2019SHZDZX01-ZX06); Shanghai Rising-Star Program (20QA1405400); Shandong Quancheng Scholarship (00242019024).

Acknowledgment. The authors sincerely thank the chief engineer Jian Tong from Shanghai Single Crystal Instrument Equipment for his strong support in helping us grow the crystal.

Disclosures. The authors declare no conflicts of interest.

Data Availability. The data that support the findings of this study are available from the corresponding author upon reasonable request.

[†] These authors contributed equally to this paper.

REFERENCES

1. N. Savage, "Ultraviolet lasers," Nat. Photonics **1**, 83–84 (2007).
2. J. Q. Meng, G. D. Liu, W. T. Zhang, L. Zhao, H. Y. Liu, X. W. Jia, D. X. Mu, S. Y. Liu, X. L. Dong, J. Zhang, W. Lu, G. L. Wang, Y. Zhou, Y. Zhu, X. Y. Wang, Z. Y. Xu, C. T. Chen, and X. J. Zhou, "Coexistence of Fermi arcs and Fermi pockets in a high-Tc copper oxide superconductor," Nature **462**, 335–338 (2009).
3. T. Sekikawa, A. Kosuge, T. Kanai, and S. Watanabe, "Nonlinear optics in the extreme ultraviolet," Nature **432**, 605–608 (2004).
4. F. D. Eaton, "Nonlinear optical materials," Science **253**, 281–287 (1991).
5. Z. Li, A. Tudi, P. Ren, Y. Yang, T. Iitaka, T. Tohyama, Z. H. Yang, S. L. Pan, and H. B. Su, "$NaPN_2$:Deep-ultraviolet nonlinear optical material with unprecedented strong second-harmonic generation coefficient," Phys. Rev. Mater. **3**, 025201 (2019).
6. Y. R. Shen, "Surface properties probed by second-harmonic and sum-frequency generation," Nature **337**, 519–525 (1989).
7. Y. L. Zhuang, X. L. Ren, X. T. Che, S. J. Liu, W. Huang, and Q. Zhao, "Organic photoresponsive materials for information storage: a review," Adv. Photon. **3**, 014001 (2021).
8. Y. F. Xiong and F. Xu, "Multifunctional integration on optical fiber tips: challenges and opportunities," Adv. Photon. **2**, 064001 (2020).
9. K. Shimamura, E. G. Villora, K. Muramatsu, and N. Ichinose, "Advantageous growth characteristics and properties of $SrAlF_5$ compared with $BaMgF_4$ for UV/VUV nonlinear optical applications," J. Cryst. Growth **275**, 128 (2005).
10. K. Shimamura, E. G. Villora, K. Takekawa, and K. Kitamura, "Ferroelectric properties and poling of $BaMgF_4$ for ultraviolet all-solid state lasers," Appl. Phys. Lett. **89**, 232911 (2006).
11. Y. L. Jia, J. L. He, H. T. Wang, S. N. Zhu, and Y. Y. Zhu, "Single pass third-harmonic generation of 310mW of 355 nm with an all-solid-state laser," Chin. Phys. Lett. **18**, 1589 (2001).
12. H. Kumagai and K. Midorikawa, "Efficient sum-frequency generation of continuous-wave single-frequency coherent light at 252 nm with dual wavelength enhancement," Opt. Lett. **28**, 1969–1971 (2003).
13. C. T. Chen, T. Sasaki, R. K. Li, Y. Wu, Z. Lin, Y. Mori, Z. Hu, J. Wang, S. Uda, M. Yoshimura, and Y. Kaneda, *Nonlinear Optical Borate Crystals: Principles and Applications* (Wiley, 2012).
14. Y. N. Xia, C. T. Chen, D. Y. Tang, and B. C. Wu, "New nonlinear optical crystals for UV and VUV harmonic generation," Adv. Mater. **7**, 79–81 (1995).
15. D. Cyranoski, "Materials science: China's crystal cache," Nature **457**, 953–955 (2009).
16. W. J. Yao, R. He, X. Y. Wang, Z. S. Lin, and C. T. Chen, "Analysis of deep-UV nonlinear optical borates: approaching the end," Adv. Opt. Mater. **2**, 411–417 (2014).
17. A. Tressaud, *Photonic and Electronic Properties of Fluoride Materials* (Elsevier Boston, 2016).
18. T. T. Tran, H. Yu, J. M. Rondinelli, K. R. Poeppelmeier, and P. S. Halasyamani, "Deep ultraviolet nonlinear optical materials," Chem. Mater. **28**, 5238–5258 (2016).
19. E. G. Villora, K. Shimamura, K. Sumiya, and H. Ishibashi, "Birefringent- and quasi phase-matching with $BaMgF_4$ for vacuum-UV/UV and mid-IR all solid-state lasers," Opt. Express **17**, 12362–12378 (2009).
20. S. M. Saltiel, D. N. Neshev, R. Fischer, W. Krolikowski, A. Arie, and Y. S. Kivshar, "Generation of second-harmonic conical waves via nonlinear Bragg diffraction," Phys. Rev. Lett. **100**, 103902 (2008).
21. R. W. Boyd, *Nonlinear Optics* (Elsevier, 2008).
22. G. A. Skripko, S. G. Bartoshevich, I. V. Mikhnyuk, and I. G. Tarazevich, "LiB_3O_5: a highly efficient frequency converter for Ti: sapphire lasers," Opt. Lett. **16**, 1726 (1991).
23. C. T. Chen, "Deep ultraviolet harmonic generation with $KBe_2BO_3F_2$ crystal," Chin. Phys. Lett. **18**, 1081 (2001).
24. S. C. Buchter, T. Y. Fan, V. Liberman, J. J. Zayhowski, and J. H. Burnett, "Periodically poled $BaMgF_4$ for ultraviolet frequency generation," Opt. Lett. **26**, 1693–1695 (2001).
25. H. R. Zeng, K. Shimamura, C. V. Kannan, E. G. Villora, S. Takekawa, and K. Kitamura, "Ferroelectric domain phenomena and microdomain engineering in $BaMgF_4$ single crystal," Appl. Phys. A **85**, 173–176 (2006).
26. L. Mateos, M. O. Ramírez, I. Carrasco, P. Molina, J. F. Galisteo-López, E. G. Víllora, C. Heras, K. Shimamura, C. Lopez, and L. E. Bausá, "$BaMgF_4$:an ultra-transparent two-dimensional nonlinear photonic

crystal with strong $\chi^{(3)}$ response in the UV spectral region," Adv. Funct. Mater. **24**, 1509–1518 (2014).

27. K. Shimamura and E. G. Villora, "Growth and characteristics of optical single crystals for UV/VUV applications," J. Fluorine Chem. **132**, 1040–1046 (2011).
28. M. Born and E. Wolf, *Principles of Optics* (Pergamon, 1980).
29. M. V. Hobden, "Phase-matched second-harmonic generation in biaxial crystals," J. Appl. Phys. **38**, 4365 (1967).